Design of a Hydraulic Ankle-Foot Orthosis

Artur Gmerek, Nader Meskin, Ehsan Sobhani Tehrani, and Robert Kearney

***Abstract*—This paper presents the design and simulation of an ankle-foot orthosis (AFO) to assist human walking. Design requirements were established based on a quantitative study of published data, simulations of human walking, and a model of intrinsic and reflex ankle joint stiffness. The design of an AFO that meets these requirements is then presented; it comprises a small linear, hydraulic actuator, a servo-valve, a hydraulic power supply, and an accumulator. Two methods of selecting the kinematic parameters of the AFO are introduced. One is based on force minimization and the other on compactness maximization. The performance expected of the AFO is demonstrated in a simulation study.**

I. Introduction

The ankle joint contributes most to walking in comparison to other redundant joints of a leg [1], but due to its high torque it is prone to injury. Every year millions of people suffer from ankle joint impairments, usually related to weakness (e.g. due to aging), and diseases such as polio, stroke, cerebral palsy and multiple sclerosis. Ten years ago the only alternative for affected people was a walking stick or a wheelchair, but recently assistive robotic orthoses have been developed to improve the life of such individuals.

Ankle-foot orthoses can be divided into two categories: passive devices, usually braces that prevent the foot from reaching certain positions; and powered AFOs that contain an actuator controlled in a manner to assist during walking. Only passive AFOs are commercially available at the present and there are concerns that their long-term usage may lead to disuse muscle atrophy [2]. This problem can be avoided by using powered AFOs which have a potential to restore the normal gait.

A comprehensive review of different AFOs can be found in [3], [4]; and it can be noticed that the most advanced AFOs are driven by an electric motor. In [5] an AFO was developed to assist ankle joint in both platarflexion-dorsiflexion and inversion-eversion directions axes. However, it cannot be used to assist ordinary patients during walking, since it is too heavy and the control system is tethered to a computer. Another example of an advanced AFO using an electric actuator is presented in [6]; this device can produce the torques as large as 97 Nm for brief periods. These AFOs have been used successfully by impaired subjects and have a great potential of development. However, the main problem for these devices is that they cannot replicate the whole spectrum of the ankle-joint properties as described in [7], [8]. This is because the relation between mass, torque, speed, response, and backdrivability in electric motors is a matter of engineering trade-off, e.g. a motor with high gear ratio can achieve high torque, but at the expense of increased mass, decreased speed of response, and backdrivability.

Consequently, many researchers have focused on fluidic AFOs using pneumatic or hydraulic actuators. Thus, in [4], [9] the AFOs were driven by pneumatic cylinders (linear and rotary respectively), while [10], [11] described AFOs driven by pneumatic muscles (PMAs). Pneumatic cylinders are faster than PMAs, but PMAs have a greater force to mass ratio. However, pneumatic actuators have a poor frequency response and so can be only used to assist patients during slow walking. Hydraulic actuators do not have this drawback, since the medium, usually oil, has a much higher bulk modulus than air. Moreover, the force to mass ratio is higher in hydraulic actuators than pneumatic ones, since the hydraulic actuators work at much higher pressures. There are only a few examples of hydraulic orthoses. One example is described in [12], where a pneumatic cylinder was filled water. A more advanced hydraulic AFO in which a small bi-directional pump drives a linear hydraulic actuator is presented in [13]. The same team later developed a special hydraulic actuator for an ankle orthosis [14].

This paper contributes to the development of the small hydraulic orthoses and prostheses. It considers the design of a hydraulic AFO including the mechanical design, hydraulic circuit design, and performances simulation.

The remainder of the paper is as follows. Section II introduces the mechanical design of the AFO including the general design, kinematic analysis, optimization of the AFO with respect to compactness and force minimization, and the CAD design. Section III presents the design of the hydraulic circuit including the consideration of different hydraulic circuits, calculation of components parameters, and a simulation study of the hydraulic system with an accumulator. The paper is discussed Sections IV, and Section V gives the conclusions.

II. AFO's design

The design requirements were established by analyzing published data of the ankle joint during normal walking, and by simulating the response of a stiffness model of the ankle joint [15]. This led to the following specifications: mean velocity of 53 $\mathrm{deg/s}$; maximum velocity of 222 $\mathrm{deg/s}$; maximum acceleration of 4715 $\mathrm{deg/s^2}$; continuous torque of 1.72 $\mathrm{Nm/kg}$; and the required minimum frequency

This publication was made possible by NPRP grant No. 6-463-2-189 from the Qatar National Research Fund (a member of The Qatar Foundation). The statements made herein are solely the responsibility of the authors.

A. Gmerek and N. Meskin are with the Department of Electrical Engineering, Qatar University, Doha, Qatar, e-mails: {*artur.gmerek*, *nader.meskin*}*@qu.edu.qa*

E. Sobhani Tehrani and R. Kearney are with the Department of Biomedical Engineering, McGill University, Montreal, QC H3A 2B4, Canada, e-mails: *ehsan.sobhani@mail.mcgill.ca*, *robert.kearney@mcgill.ca*

bandwidth of 7 Hz. Thus, taking the average weight of humans, to 63 kg, the actuator should create the torque of 108 Nm. We assumed that half of the required force would be provided by the patient, so that the AFO should produce a continuous torque of 50 Nm. This is a high torque requirement for an electric actuator that would be light enough to mount on a subject's leg. Moreover, the frequency bandwidth of 7 Hz is usually too high for a pneumatic actuator. Therefore, hydraulic actuator was selected, and the AFO is designed in terms of both the mechanical structure and hydraulic circuit.

The main challenge in designing a hydraulic AFO is finding components with the required specifications. Hydraulic components are usually produced for the high-power industry, and only a few small hydraulic components are available. Indeed, we could not find a rotary hydraulic motor which fit our requirements. The design of a rotary actuator is more complicated than a linear cylinder, consequently we focused on the design of a linear hydraulic AFO. The cylinder could be placed on the back of a shank and connected to a foot part of AFO via a lever, alternatively, it could be mounted on the front of the shank, and connected to collar on the orthosis. We chose to mount the hydraulic cylinder on the back of the shank since this solution is more anthropometric, and aesthetics is important to patients. Figure 1 shows the kinematic structure of the envisioned AFO; it is a closed-loop chain consisting of one active prismatic joint between two passive rotary joints.

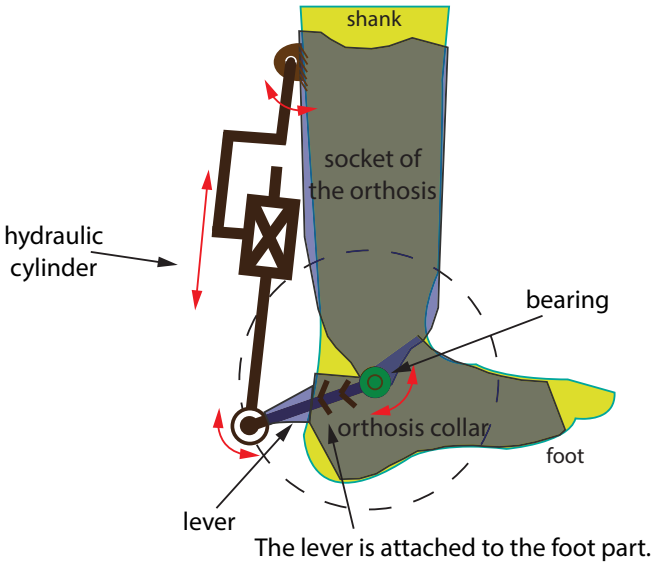

Fig. 1. The general kinematic design of the AFO.

A. The geometry of the piston rod

It is planned to mount a hydraulic actuator on the back of a leg and to transmit force via a lever. Consequently, higher forces will be produced in the dorsiflexion direction than the plantarflexion direction if using a standard single rod actuator. This is not consistent with the anthropomorphic characteristic of a human body where the higher torques are produced in plantarflexion. To compensate for this, it is possible to manufacture a special rod with different diameters of the piston rod in each chamber which is presented in Figure 2. Moreover, this configuration makes it possible to limit the maximum and minimum positions via simple safety nuts which can be placed on either side of the piston rod.

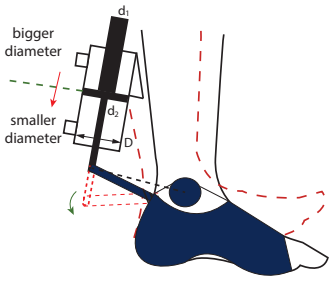

Fig. 2. Visualization of the double piston rod with unequal active areas to meet the anthropometric criterion of an ankle joint's torque characteristic.

The force in the plantarflexion direction is:

$$F = A_1 p_1 - A_2 p_2, \tag{1}$$

where A_1 is the active area of the top side of the cylinder, and p_1 is the pressure in the upper chamber, A_2 is the active area of the bottom of the cylinder, and p_2 is the pressure in the bottom chamber. The active areas are given by:

$$A_1 = \frac{\pi}{4}(D^2 - d_1^2), \tag{2}$$

$$A_2 = \frac{\pi}{4}(D^2 - d_2^2), \tag{3}$$

where D is the cylinder bore, d_1 and d_2 are the diameters of an upper and bottom side of a piston rod.

B. The geometry of the AFO in the sagittal plane

Only the sagittal plane design of the AFO is considered. The kinematic equations are derived assuming that the orthosis is driven by a linear hydraulic cylinder mounted on the back of a shank. The actuator transfers force via a lever, and the cylinder is fastened to the constant point on the orthosis' socket with coordinate $(-g, s)$ as is presented in Figure 3, where:

- g is the horizontal distance between the ankle and the attachment point,
- s is the vertical distance between the middle point of a shank and the center of the ankle and the origin of the coordinate system is located at the ankle joint,
- l is the length of the lever starting from the ankle joint,
- θ is the angle of connection between the socket and the hydraulic cylinder,
- a is the minimum length from the attachment point of the cylinder barrel to the lever (minimum stroke),
- b is the maximum length of a cylinder from the attachment point of the cylinder barrel to the lever (with max. stroke),
- d is the arbitrary selected length from the attachment point of the cylinder barrel to the lever,

- α_d denotes the maximum dorsiflexion angle,
- α_p denotes the maximum plantarflexion angle,
- the stroke of the cylinder equals $b-a$.

In this configuration, the piston rod is completely hidden in the plantarflexion position, and the tip of the cylinder barrel does not need to be connected to the vertical attachment point s (the barrel can be connected below its tip). The kinematic relationship between the angle α and the current length of the cylinder d is needed to calculate the linear position corresponding to the current ankle joint angle. This relationship is:

$$d^2 = l^2 + g^2 + s^2 - 2l\sqrt{g^2+s^2}\cos(\rho+\alpha). \quad (4)$$

Recognizing that $\rho = 90 - \delta$ with $\delta = \operatorname{atan}(\frac{g}{s})$, α can be expressed as:

$$\alpha = \operatorname{acos}(\frac{l^2+g^2+s^2-d^2}{2l\sqrt{g^2+s^2}}) - 90^\circ + \operatorname{atan}(\frac{g}{s}). \quad (5)$$

It should be recognized that the angle β between the position vector and the force vector changes during movement. Accordingly, the torque depends on the force and the angle between the position and the force vector as:

$$\tau = Fl\sin(\beta) = Fl\sin(90-\alpha-\theta) = Fl\cos(\alpha+\theta), \quad (6)$$

and the relationship between the linear velocity of the piston rod, and the angular speed is:

$$v = \frac{l\omega}{\sin(\beta)}. \quad (7)$$

Moreover, it follows that

$$\beta + \theta + \alpha = 90^\circ. \quad (8)$$

Using the cosine theorem on $\triangle$ABC, it can be obtained:

$$l^2 = d^2 + g^2 + s^2 - 2d\sqrt{g^2+s^2}\cos(\theta + \operatorname{atan}\frac{g}{s}). \quad (9)$$

Therefore:

$$\theta = \operatorname{acos}(\frac{d^2+g^2+s^2-l^2}{2d\sqrt{g^2+s^2}}) - \operatorname{atan}(\frac{g}{s}), \quad (10)$$

and consequently, by substituting (5) and (10) to (8), the angle β can be written as:

$$\beta = 180^\circ - \operatorname{acos}(\frac{d^2+g^2+s^2-l^2}{2d\sqrt{g^2+s^2}}) - \operatorname{acos}(\frac{l^2+g^2+s^2-d^2}{2l\sqrt{g^2+s^2}}), \quad (11)$$

where d can be measured with the use of a linear potentiometer.

C. Optimization of the kinematic design

The aim of the optimization is to select the geometric parameters of the AFO which meet two separate criteria: the maximization of compactness; and the minimization of the required force. The optimization procedure is performed by using exhaustive search on two kinematic equations which describe the AFO's kinematic arrangements in the maximum and minimum positions. These equations can be derived using the cosine theorem on $\triangle$ADO and $\triangle$ABO as follows:

$$\begin{cases} a^2 = g^2+s^2+l^2-2l\sqrt{g^2+s^2}\cos(\operatorname{atan}(\frac{s}{g})+\alpha_p) \\ b^2 = g^2+s^2+l^2-2l\sqrt{g^2+s^2}\cos(\operatorname{atan}(\frac{s}{g})+\alpha_d) \end{cases}. \quad (12)$$

These equations can be simplified using common trigonometric identities on cosine of the sum of angles, and based on the relationship between simple and inverse trigonometric functions. The following set of equations results:

$$\begin{cases} -a^2+g^2+s^2+l^2+2l(s\cdot\sin(\alpha_p)-g\cdot\cos(\alpha_p)) = 0 \\ -b^2+g^2+s^2+l^2+2l(s\cdot\sin(\alpha_d)-g\cdot\cos(\alpha_d)) = 0 \end{cases}, \quad (13)$$

where α_p is negative.

The optimization procedure is to find the optimal values of the: lever length (l), the cylinder stroke $b-a$, the vertical attachment point of the cylinder barrel (s), the maximum (θ_{plant}) and minimum (θ_{dorsi}) angles (needed for the proper cylinder mounting), and the maximum force required from the actuator ($F_{\max}$). It was assumed that the horizontal distance between the hydraulic cylinder's fixation point and the ankle equals $g = 7$ cm (this parameter depends on the thickness of a leg and geometry of a socket). Since the cylinder diameter was not included in the analysis, the g-parameter must be selected to ensure correct mounting of cylinders with larger diameters. This value was selected based on the observation of the geometry of a leg in an adult male subject and pre-assumptions about the orthosis' socket. Based on the range of foot's motion in most subjects the maximum required plantarflexion angle equals -50° and the maximum dorsiflexion angle equals 30°.

D. Compactness

The compactness criterion comes from the assumption that since the orthosis is a wearable device, it should be as small and light as possible. Consequently, unknown parameters were initially selected to minimize of the lever length and cylinder stroke. The procedure was to select the smallest lever length (l) and then calculate the other parameters using (13). The orthosis socket must be at least 15 cm above the ankle joint for the orthosis to generate the required maximum torque. Moreover, the minimum length of the smallest, available cylinder barrel was $5.1\text{ cm} + Stroke$ (Parker CHE cylinders [16]). Hence, the vertical point of the cylinder attachment in this optimization criterion was chosen as $s = 15$ cm. The geometric constraints limit the lever length to be no less than the distance from the ankle joint to a tip of the heel (approximately g). Conversely, the lever cannot be too long, or it would hit the ground during walking. Taking these limits into account the lever length is bounded by:

$$g < l < 20\text{ cm}. \quad (14)$$

This analysis does consider the cylinder diameter, and consequently the g parameter might need to be increased for large cylinder diameters. This analysis used smallest available cylinder with a bore size of 20 mm (e.g. Parker CHE 20-K-T-CHE-3-T–9-4A-50) and so there was not need to modify g. Figure 4 presents visualization of the optimization procedure. The small solid circles and large dashed circles

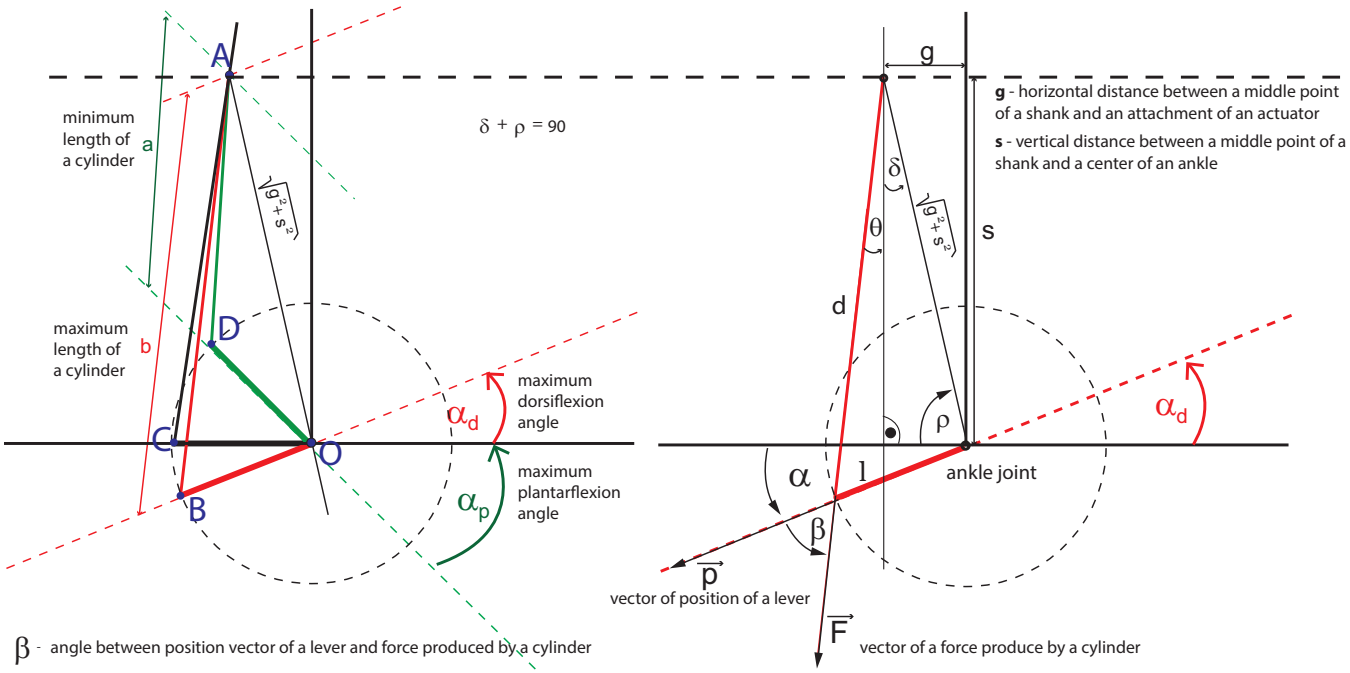

Fig. 3. The geometric relationship of the AFO.

around the attachment point $(-g, s)$ show the virtual path of the cylinder (in shortest and longest piston rod position). The circles centered at (0,0) show the lever path. The points of intersections between circles of the same color denote the minimum and the full stroke. The parameter selected for the shortest lever length (7 cm) were:

$$\begin{aligned} g &= 7 \text{ cm}, \\ s &= 15 \text{ cm}, \\ a &= 9.95 \text{ cm}, \\ b &= 18.52 \text{ cm}, \\ Stroke &= 8.6 \text{ cm}, \\ l &= 7 \text{ cm}, \\ \theta_{\text{plant}} &= -14.63°, \\ \theta_{\text{dorsi}} &= -2.89°, \\ F_{\max} &= 1.68 \text{ kN}. \end{aligned} \tag{15}$$

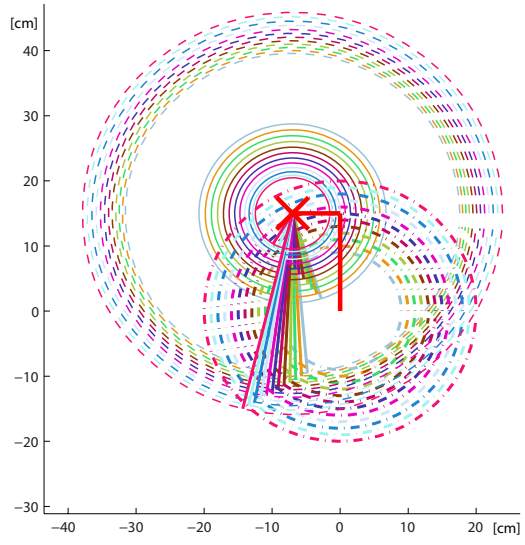

Fig. 4. Visualization of the compactness optimization algorithm.

The orthosis is small-sized but the force requirement is large. Figure 5 shows the AFO structure for these parameters.

E. Force minimization

To minimize the force requirement for the actuator, the optimization procedure was based on the force-torque relation:

$$F = \frac{\tau}{l \sin(\beta)}. \tag{16}$$

Accordingly, the minimum absolute force requirements will be achieved by maximizing l and $\sin(\beta)$. The maximum length of a lever is 20 cm to prevent it from touching ground. Choosing the correct values of l requires an iterative optimization because l and β are coupled according to (11). Figure 6 shows the results obtained for various values of l and β. The shorter the lever the greater the force that must be applied to produce the required torque, and the greater the range of forces that must be applied. Increasing the lever length beyond 13 cm does not significantly change the maximum needed force. Accordingly, 13 cm was selected for the lever length resulting in the other parameter values

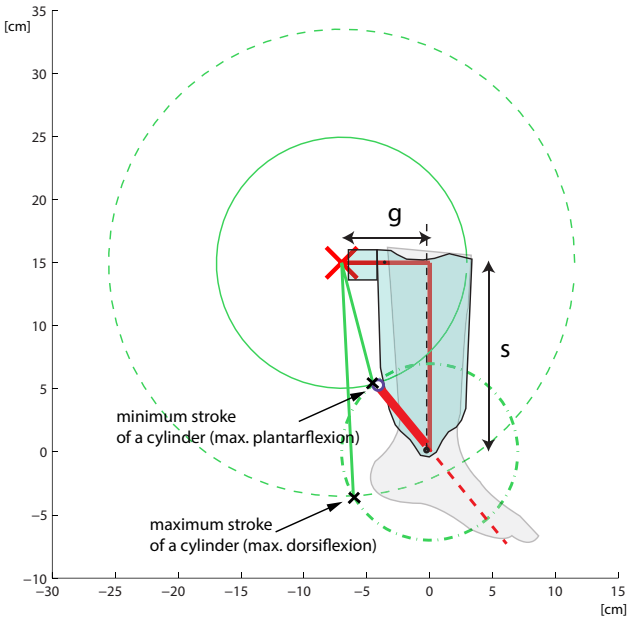

Fig. 5. The geometry of an AFO optimised for compactness.

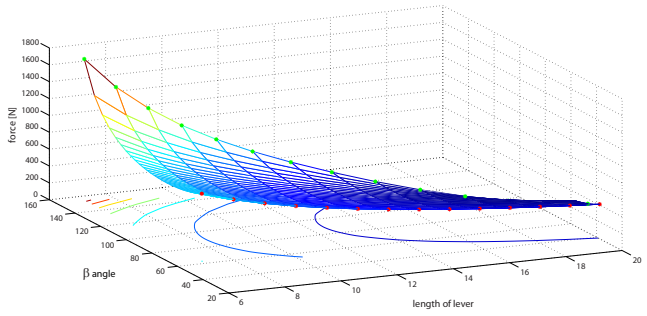

Fig. 6. The relationship between force (F), angle β, and the length of the lever (l) of the envisioned AFO.

of:

$$\begin{aligned} g &= 7 \text{ cm}, \\ s &= 15 \text{ cm}, \\ a &= 5.21 \text{ cm}, \\ b &= 21.92 \text{ cm}, \\ Stroke &= 16.7 \text{ cm}, \\ l &= 13 \text{ cm}, \\ \theta_{\text{plant}} &= 15°, \\ \theta_{\text{dorsi}} &= 11.2°, \\ F_{\max} &= 0.51 \text{ kN}. \end{aligned} \tag{17}$$

In this situation the special attention must be taken when using a double-rod cylinder to prevent the upper end of a piston rod from contacting with a shank at the maximum angle of $15°$. This can be prevented by increasing g parameter.

Figure 7 shows the CAD design of an AFO with these parameters. For this configuration, the AFO will be built from two types of plastic: PLA (deep blue color) and flexible polyester-based filaments (transparent blue color). The shape of the plastic parts includes cut-outs to permit the attachment of EMG electrodes on the calf muscles. The AFO also incorporates an adjusted hinge joint at the ankle joint to prevent the shank part of the AFO from moving on the surface of the patient's skin.

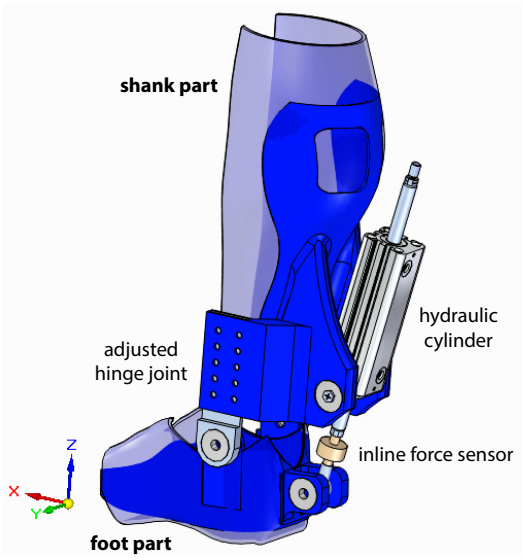

Fig. 7. CAD design of the hydraulic AFO.

III. Hydraulic Circuit

A hydraulic system usually consists of: a hydraulic pump, a primary mover to drive a pump (e.g. an electric motor) together with a controller, a servo valve with a controller, a hydraulic actuator, a reservoir with a filter and sometimes a cooler, check and relief valves, a hydraulic accumulator, a manifold to mount hydraulic components, hoses and connectors, a battery pack to power the equipment, and additional sensors such as flow sensor, pressure sensor, position and force sensors. Many of these elements can be purchased in one, ready to use unit (so called - a *power unit*) consisting of a pump, a reservoir, a filter, as well as check and relief valves.

The hydraulic circuit for the AFO was chosen based on the following requirements:

- It should provide sufficient flow rate and pressure to drive the actuator with the desired torque, speed, acceleration, and frequency response;
- The whole system should be wearable which means that it should be also as light as possible and the components-orientation can be changed. This is important since many pumps only work in the horizontal or vertical positions;
- The system should be easy to manufacture and environmentally friendly.

Figure 8 shows the closed-loop circuit, hydraulic system we selected best meets these requirement. However, problem with this hydraulic circuit is that to generate the high torque and speed needed would require a large hydraulic pump and consequently to a high-power motor. This could be

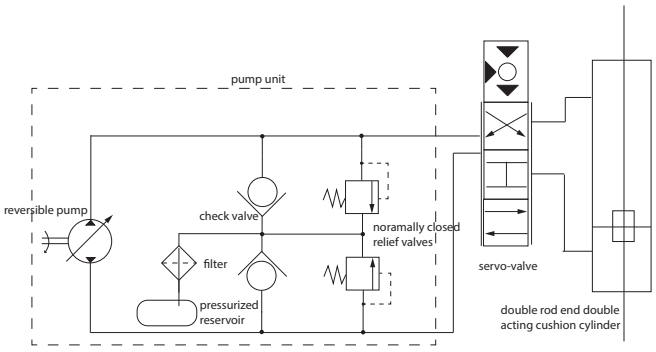

Fig. 8. A closed-loop hydraulic circuit with a bi-directional pump.

partially overcome by using a hydraulic accumulator where fluid is kept under pressure, by a mass, internal spring, or a bladder/diaphragm filled with a gas. The accumulator stores and releases fluid under pressure. One problem with using a reversible pump in a hydraulic closed loop system is that two accumulators would be required. Consequently, we will consider only a unidirectional hydraulic circuit as presented in Figure 9. It should be noticed that an accumulator will

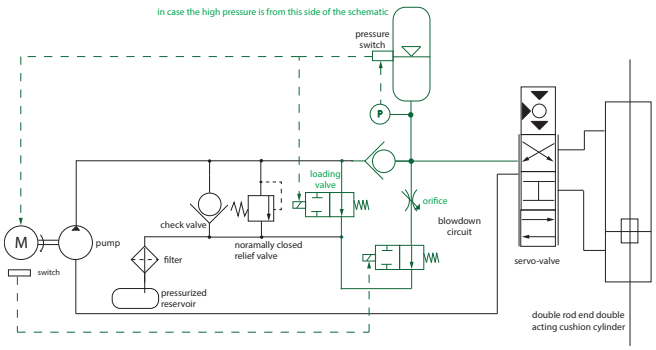

Fig. 9. A closed-loop hydraulic circuit with an accumulator.

not reduce the pump requirement in case that a continuous operation is required and a standard bi-directional valves are used, since there will be no time to charge it. However, when using a servo-valve and the control signal is periodic, then the situation is different, due to the fact that the fluid is partially pressurized by the servo-valve's nozzle. Hence, the pump can be sized based on the mean absolute flow requirement.

A. Calculation of the hydraulic system parameters

In this subsection the parameters of the hydraulic system are calculated in order demonstrate how to size the hydraulic components for the AFO. It is assumed that the safety factor equals $\eta = 1$, therefore the force requirements already included friction and all uncertain counter-forces. The hydraulic system is sized for the AFO' parameters obtained from the force minimization procedure with a lever length of 13 cm, and cylinder stroke is 17 cm.

For a required torque of $\tau = 50$ Nm, the *nominal force* of a hydraulic cylinder becomes:

$$F = \frac{\tau}{l\sin\beta_{\min}} = \frac{50}{0.13\cdot 0.4} \approx 510 \text{ N}, \tag{18}$$

where $\beta_{\min}$ is the minimum angle of β for the selected configuration (the worse case scenario).

The *maximum linear velocity* of a piston rod can be calculated based on the required speed ($222\frac{\text{deg}}{\text{s}} = 3.87\ \frac{\text{rad}}{\text{s}}$), by using the following formula:

$$v_{\text{lin}} = \frac{l\omega}{\sin\beta_{\min}} = \frac{0.13\cdot 3.87}{0.754} = 0.67\ \frac{\text{m}}{\text{s}} = 67\ \frac{\text{cm}}{\text{s}}, \tag{19}$$

where ω is the required angular speed. The *working pressure* is chosen *a priori* by examining the available components, hence, a pressure of $P = 200$ bar $=$ 20 MPa is selected here.

The *active area of a cylinder* can be calculated from the required force and working pressure as

$$A = \frac{F}{P} = \frac{510}{20\cdot 10^6} = 0.25 \text{ cm}^2. \tag{20}$$

It is then possible to calculate the dimension of the piston rod and the bore diameter. The equation of the area of an annulus surface is:

$$A = \frac{(D^2 - d^2)\pi}{4}, \tag{21}$$

where A is an active area of a cylinder, D is a bore diameter, and d is diameter of a piston rod. Accordingly, D and d are related as:

$$\frac{4A}{\pi} = D^2 - d^2 = 0.33 \text{ cm}^2. \tag{22}$$

They can be selected as: $d = 1.2$ cm and $D = 1.235$ cm.

The corresponding *flow rate* can be calculated as:

$$Q = v_{\text{lin}}A = 67\ \frac{\text{cm}}{\text{s}}\cdot 0.25 \text{ cm}^2 = 17\ \frac{\text{cm}^3}{\text{s}}, \tag{23}$$

where v_{lin} is the required maximum linear speed, and A is the cylinder active area. If a hydraulic circuit with the accumulator is used then this maximum calculated flow requirement is the required servo-valve flow. The *flow produced by a pump* (Q_{p}) can be calculated based on the mean velocity requirement (53 deg/s) as $Q_{\text{p}} = 4$ cm^3/s. This flow can be used to further calculate the *displacement of a pump* (D_{pump}). By considering the rotation speed of the motor as $n = 3000\ \frac{\text{rev}}{\text{min}} = 50\ \frac{\text{rev}}{\text{s}}$, the resulting pump displacement is:

$$D_{\text{pump}} = \frac{Q}{n\zeta} = \frac{4\ \frac{\text{cm}^3}{\text{s}}}{50\ \frac{\text{rev}}{\text{s}}\cdot 0.9} = 0.09\ \frac{\text{cm}^3}{\text{rev}}, \tag{24}$$

where ζ is the volumetric efficiency of the pump. In this case the *torque to drive the pump* (τ_{pump}) becomes:

$$\tau_{\text{pump}} = \frac{D_{\text{pump}}P}{2\pi\eta_{\text{mech}}} = \frac{0.09\cdot 10^{-6}\cdot 20\cdot 10^6}{6.28\cdot 0.9} \approx 0.318 \text{ Nm}, \tag{25}$$

where η_{mech} is the pump's mechanical efficiency. Finally, the *motor power required to drive the hydraulic pump* (W) is:

$$W = \tau_{\text{pump}}n = 0.318 \text{ Nm}\cdot 50\cdot 2\pi\ \frac{\text{rad}}{\text{s}} = 367 \text{ Watt}. \tag{26}$$

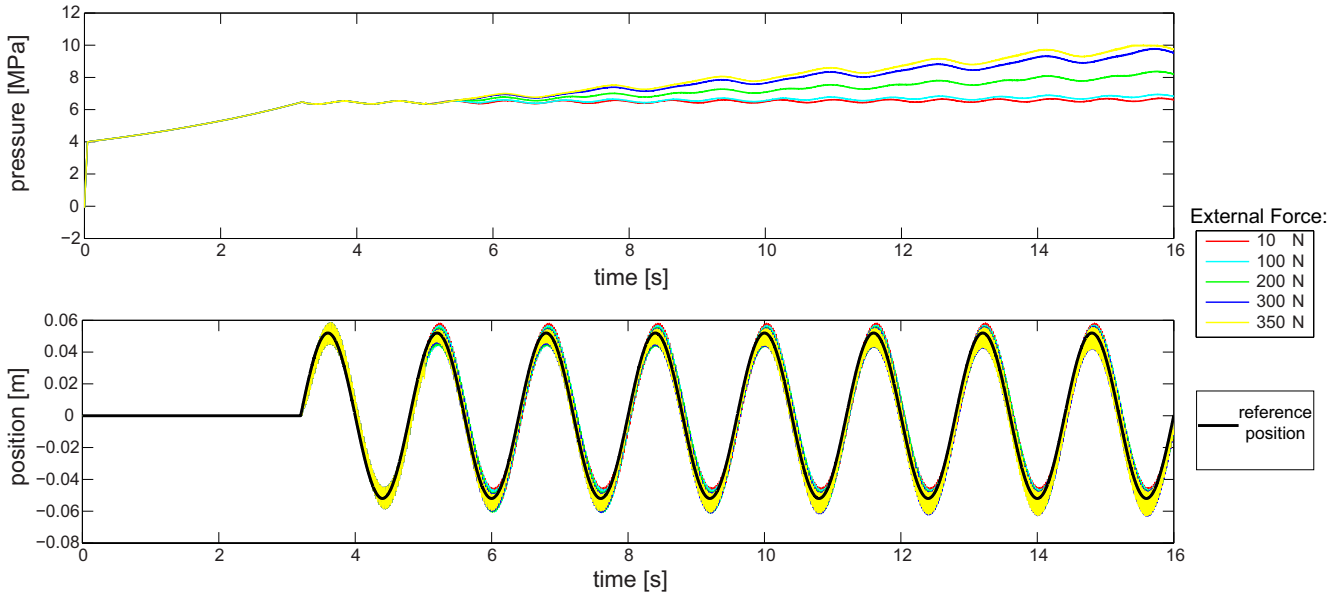

Fig. 10. The time history of the pressure and the cylinder rod position of the hydraulic circuit with an accumulator for different values of external force acting on the actuator.

B. Simulation study

A simulation study was conducted to examine this performance of a hydraulic system comprising a servo-valve, an accumulator and a pump size on the mean absolute velocity of a periodic control signal. The hydraulic circuit shown in Figure 9 was modeled and simulated in Matlab Simhydraulics. The system was controlled using an PID controller, and the desired control trajectory was a sinusoid with known velocity. The mean absolute velocity of the sinusoid was used to size the pump ($Q_{\mathrm{p}} = A \cdot v_{\mathrm{mean\ abs}}$). The hydraulic accumulator was charged before starting the periodic trajectory. If the system does not have enough flow then it will be only able to track the desired trajectory in the initial phase of operation using oil stored in the accumulator. However, the simulation study showed that the system accurately tracks the desired trajectory for long periods of time. To examine this phenomena, the experiment was repeated for various external forces as is presented in Figure 10 which depicts the pressure and position as functions of time. Analysis of the system behavior reveals that the accumulator was charged when the servo-valve spool was near the center of the valve while it traveled from one side to another (due to periodicity of the reference signal). As such times the internal hydraulic resistance of the system is high causing it to pressurize the fluid and recharge the accumulator. If the force is higher, then the internal resistance is also respectively higher which permits the system pressure to be maintained almost constant. The simulation study also revealed one of drawback of this configuration that when the pre-charged pressure of an accumulator is high then the system might suffer from the internal pressure fluctuations.

IV. Discussion

This research outlines the steps involved in the development of the hydraulic AFO. Two kinematic optimization procedures were introduced: one which results in a compact AFO and a second which yields a larger AFO with a lower actuator force requirement. The mechanical structure and hydraulic circuit we chose resulted in a small actuator and a small power unit. The possibility of using a compact power unit is based on the phenomena that in the hydraulic circuit with an accumulator and a servo-valve, when a desired trajectory consists of a swing phase of walking during which the accumulator can recharge, the pump can be selected based on the mean absolute velocity. Otherwise, the required flow must to be calculated based on the maximum required velocity, which results in a much larger power-unit.

Such a small power unit could be carried in the backpack by a patient, and there are companies on the market that can provide such a hydraulic pumps off-the-shelf. However, the study also demonstrates that such an AFO would require building a new hydraulic cylinder; the smallest available actuator on the market has a piston rod diameter of 12 mm and a bore diameter of 20 mm [16]. Selecting larger actuator is not desirable since it increases the flow requirements and results in a bigger pump unit. Unfortunately, building such an actuator is difficult since it requires creating the special tailored sealed system that is difficult to manufacture and miniaturize. A pilot study of such an actuator can be found in [14], [17] although neither the exact characteristic of the actuator nor a control algorithm has been provided.

V. Conclusions

The paper presents the design of the hydraulic ankle-foot orthosis which is be able to provide 50 Nm of torque with a maximum angular velocity of 222 $\mathrm{deg/s}$ in the sagittal

plane. A kinematic model of the AFO was derived for an actuator mounted on the back of the shank, and two methods of the AFO's mechanical parameters selection were presented based on the compactness maximization and a second based on the force minimization. The AFO is driven by a closed-loop hydraulic circuit with an accumulator that could lower the requirements in relation to a pump and prevent energy waste. The AFO would be wearable and lightweight - the foot part would weight about 0.5 kg, and the power unit without battery would weight approximately 3 kg. The hydraulic system should also meet the frequency response requirements according to the servovalve specifications. The paper presents the detailed procedure for deriving the AFO's kinematics, sizing the hydraulic components, and the simulation study of the hydraulic circuit with a simple position controller. The system has not been tested yet in the real life, since the market research of the available hydraulic components suggest that design requires a hydraulic cylinder with characteristics not currently available.

REFERENCES

[1] K. E. Zelik, K. Z. Takahashi, and G. S. Sawicki, "Six degree-of-freedom analysis of hip, knee, ankle and foot provides updated understanding of biomechanical work during human walking," *The Journal of experimental biology*, vol. 218, no. 6, pp. 876–886, 2015.

[2] J. F. Geboers, M. R. Drost, F. Spaans, H. Kuipers, and H. A. Seelen, "Immediate and long-term effects of ankle-foot orthosis on muscle activity during walking: A randomized study of patients with unilateral foot drop," *Archives of Physical Medicine and Rehabilitation*, vol. 83, no. 2, p. 240245, Feb 2002.

[3] M. Hamedi, P. Salimi, A. Aliabadi, and M. Vismeh, "Toward intelligent ankle foot orthosis for foot-drop, a review of technologies and possibilities," in *Biomedical Engineering (ICoBE), 2015 2nd International Conference on*, 2015, pp. 1–5.

[4] K. Shorter, J. Xia, E. Hsiao-Wecksler, W. Durfee, and G. Kogler, "Technologies for powered ankle-foot orthotic systems: Possibilities and challenges," vol. 18, no. 1, pp. 337–347, 2013.

[5] A. Roy, H. Krebs, D. Williams, C. Bever, L. Forrester, R. Macko, and N. Hogan, "Robot-aided neurorehabilitation: A novel robot for ankle rehabilitation," vol. 25, no. 3, pp. 569–582, 2009.

[6] S. Hwang, J. Kim, J. Yi, K. Tae, K. Ryu, and Y. Kim, "Development of an active ankle foot orthosis for the prevention of foot drop and toe drag," in *Biomedical and Pharmaceutical Engineering, 2006. ICBPE 2006. International Conference on*, 2006, pp. 418–423.

[7] G. Luo and D. Stefanyshyn, "Limb force and non-sagittal plane joint moments during maximum-effort curve sprint running in humans," *The Journal of experimental biology*, vol. 215, no. 24, pp. 4314–4321, 2012.

[8] M. Mirbagheri, H. Barbeau, and R. Kearney, "Intrinsic and reflex contributions to human ankle stiffness: variation with activation level and position," *Experimental Brain Research*, vol. 135, no. 4, pp. 423–436, 2000.

[9] S.-K. Wu, M. Jordan, and X. Shen, "A pneumatically-actuated lower-limb orthosis," in *Engineering in Medicine and Biology Society, EMBC, 2011 Annual International Conference of the IEEE*, 2011, pp. 8126–8129.

[10] Y.-L. Park, B. rong Chen, D. Young, L. Stirling, R. J. Wood, E. Goldfield, and R. Nagpal, "Bio-inspired active soft orthotic device for ankle foot pathologies," in *Intelligent Robots and Systems (IROS), 2011 IEEE/RSJ International Conference on*, 2011, pp. 4488–4495.

[11] C. Teng, Z. Wong, W. Teh, and Y. Z. Chong, "Design and development of inexpensive pneumatically-powered assisted knee-ankle-foot orthosis for gait rehabilitation-preliminary finding," in *Biomedical Engineering (ICoBE), 2012 International Conference on*, 2012, pp. 28–32.

[12] M. Noel, B. Cantin, S. Lambert, C. Gosselin, and L. Bouyer, "An electrohydraulic actuated ankle foot orthosis to generate force fields and to test proprioceptive reflexes during human walking," *IEEE Transactions on Neural Systems and Rehabilitation Engineering*, vol. 16, no. 4, pp. 390–399, Aug 2008.

[13] K. L. Houle, "A power transmission design for an untethered hydraulic ankle orthosis," Master's thesis, THE UNIVERSITY OF MINNESOTA, 2012.

[14] B. Neubauer, J. Nath, and W. Durfee, "Design of a portable hydraulic ankle-foot orthosis," in *Engineering in Medicine and Biology Society (EMBC), 2014 36th Annual International Conference of the IEEE*, 2014, pp. 1182–1185.

[15] D. Ludvig, T. Visser, H. Giesbrecht, and R. Kearney, "Identification of time-varying intrinsic and reflex joint stiffness," *IEEE Transactions on Biomedical Engineering*, vol. 58, no. 6, pp. 1715–1723, 2011.

[16] Parker Hannifin Corporation - hydraulics manufacturer. [Online]. Available: www.parker.com

[17] W. Durfee, J. Xia, and E. Hsiao-Wecksler, "Tiny hydraulics for powered orthotics," in *Rehabilitation Robotics (ICORR), 2011 IEEE International Conference on*, 2011, pp. 1–6.